

QERA: an Analytical Framework for Quantization Error Reconstruction

Cheng Zhang*, Jeffrey T. H. Wong†, Can Xiao‡ and George A. Constantinides§ Yiren Zhao¶

Department of Electrical and Electronic Engineering, Imperial College London

London, UK

Email: *cheng.zhang122@imperial.ac.uk, †tsz.wong20@imperial.ac.uk,

‡can.xiao22@imperial.ac.uk, §g.constantinides@imperial.ac.uk, ¶a.zhao@imperial.ac.uk

Abstract

The growing number of parameters and computational demands of large language models (LLMs) present significant challenges for their efficient deployment. Recently, there is an increasing interest in quantizing weights to extremely low precision while offsetting the resulting error with low-rank, high-precision error reconstruction terms. The combination of quantization and low-rank approximation is now popular in both adapter-based, parameter-efficient fine-tuning methods such as LoftQ [1] and low-precision inference techniques including ZeroQuant-V2 [2]. Usually, the low-rank terms are calculated via the singular value decomposition (SVD) of the weight quantization error, minimizing the Frobenius and spectral norms of the weight approximation error. Recent methods like LQ-LoRA [3] and LQER [4] introduced hand-crafted heuristics to minimize errors in layer outputs (activations) rather than weights, resulting improved quantization results.

However, these heuristic-based methods lack an analytical solution to guide the design of quantization error reconstruction terms. In this paper, we revisit this problem and formulate an analytical framework, named Quantization Error Reconstruction Analysis (QERA), and offer a closed-form solution to the problem. We show QERA benefits both existing low-precision fine-tuning and inference methods – QERA achieves a fine-tuned accuracy gain for $\Delta_{\text{acc}} = 6.05\%$ of 2-bit RoBERTa-base on GLUE compared to LoftQ; and obtains $\Delta_{\text{acc}} = 2.97\%$ higher post-training quantization accuracy of 4-bit Llama-3.1-70B compared to ZeroQuant-V2 and $\Delta_{\text{ppl}} = -0.28$ lower perplexity on WikiText2 compared to LQER.

Index Terms

LLMs, low-rank approximation, parameter-efficient fine-tuning, post-training quantization

I. INTRODUCTION

The demand for efficient deployment of large language models (LLMs) has been increasing [5]. LLMs now typically contain billions of parameters [6, 7], making their fine-tuning and inference computationally expensive and resource-intensive [8]. To address these challenges, there has been a surge of interest in building efficient fine-tuning and inference methods. One popular formulation is to apply a low-rank term to reconstruct the error after quantization. Given a linear layer $y = xW$, the weight matrix $W \in \mathbb{R}^{m \times n}$ is quantized to \tilde{W} , and we rewrite $W \approx \tilde{W} + A_k B_k$ such that both A_k and B_k are low-rank yet high-precision terms with rank $k \ll \min(m, n)$.

We call the problem of finding the optimal A_k and B_k *quantization error reconstruction*. Interestingly, this problem has, coincidentally, seen widespread application in two actively researched areas: quantized parameter-efficient fine-tuning (QPEFT) and post-training quantization (PTQ) for model inference. QPEFT refers to fine-tuning techniques that adapt LLMs to specific tasks by quantizing pretrained weights and updating only a small number of extra parameters, hence significantly reducing memory requirements and training time, such as QLoRA [3]. On the other side, PTQ is a training-free method that reduces the model size and may accelerate the forward pass if the underlying hardware supports it. Recently, researchers combined PTQ with quantization error reconstruction [2, 9, 4] to further reduce weight precision. Works such as ZeroQuant-V2 [2] and LQER [4] have shown that adding a high-precision low-rank component, as low as 8 or 32, can recover considerable model performance for 3- or 4-bit weight quantization.

Although both the QPEFT and PTQ methods have demonstrated substantial performance improvements in lowering the computational overhead of LLMs, a theoretical analysis of quantization error reconstruction is lacking. Usually, A_k and B_k are calculated by applying truncated singular value decomposition (SVD) to the weight quantization error ($W - \tilde{W}$), minimizing the Frobenius and spectral norms of the *weight approximation error*. However, recent work on activation-aware quantization and knowledge distillation implies that minimizing *layer output error* generally leads to a greater performance gain than minimizing weight approximation error [10, 9, 11].

Besides the unsettled minimization objective, it has remained unclear whether there exists a theoretically optimal solution for the values of A_k and B_k , and if so, how one can solve for it. A better initialization or theoretically grounded initialization of A_k and B_k brings direct benefits for both QPEFT and PTQ. In QPEFT, the initialization of LoRA [12], which uses element-wise Gaussian random values for A_k and zeros for B_k , struggles under aggressive quantization since the quantization error

can derail fine-tuning. In PTQ, the quantized model performance is based on the computation of the low-rank terms, given a specific quantization function $q(\cdot)$ and rank k .

In this paper, we aim to provide an analytical framework for the *quantization error reconstruction* problem. To demonstrate the effectiveness of our theoretical framework, we further apply our analytical solutions to state-of-the-art QPEFT and PTQ methods and show the significant performance improvements under the same computational budget. Specifically, our contributions are as follows:

- We show that the commonly used objective for solving the *quantization error reconstruction* problem in prior work [], *i.e.*, minimizing the weight approximation error (*e.g.*, $\|\mathbf{W} - \widetilde{\mathbf{W}}\|_p$), does not guarantee a reduced *model output error*. Instead, we show that minimizing the layer output error (*e.g.*, $\|\mathbf{y} - \widetilde{\mathbf{y}}\|_p$) is closely related to minimizing the model output error.
- We derive the analytical solution to the low-rank terms \mathbf{A}_k and \mathbf{B}_k by minimizing the layer output error. We demonstrate that under a statistical assumption, this solution can be found in a particularly computationally efficient manner, also explaining the success of LQER.
- We empirically demonstrate the effectiveness of our solutions by applying them to state-of-the-art QPEFT and PTQ methods. Our analytical framework, QERA, significantly improves the performance of these methods. For example, QERA achieves $\Delta_{\text{acc}} = 6.05\%$ higher accuracy of 2-bit RoBERTa-base on GLUE compared to LoftQ, improving the fine-tuning accuracy and efficiency. Moreover, QERA obtains $\Delta_{\text{acc}} = 2.97\%$ higher accuracy than ZeroQuant-V2, when quantizing LLaMA-3-70B to 4 bits, averaged across six tasks. This narrows the model performance gap between error-reconstruction-based post-training quantization and full-precision models.

II. RELATED WORK

In this section, we review the existing methods that combine weight quantization and low-rank error reconstruction. These methods can be roughly categorized into two groups based on their applications: QPEFT for training and PTQ for inference.

a) *LoRA and QPEFT*: LoRA [12] is a representative PEFT method that introduces trainable low-rank terms to adapt the model to a specific task. Take a linear layer as an example,

$$\mathbf{y} = \mathbf{x}(\mathbf{W} + \mathbf{A}_k \mathbf{B}_k) \quad (1)$$

where $\mathbf{W} \in \mathbb{R}^{m \times n}$ is the pretrained weight matrix, row vector $\mathbf{x} \in \mathbb{R}^m$ and $\mathbf{y} \in \mathbb{R}^n$ are the input and output, and $\mathbf{A}_k \in \mathbb{R}^{m \times k}$ and $\mathbf{B}_k \in \mathbb{R}^{k \times n}$ are trainable low-rank matrices (“adapter”) with rank $k \ll \min(m, n)$. During fine-tuning, the pretrained \mathbf{W} is frozen and only the adapter \mathbf{A}_k and \mathbf{B}_k are updated. To make the adapted layer’s output match the original one at the start of fine-tuning, LoRA initializes \mathbf{A}_k with Gaussian random values and \mathbf{B}_k with zeros. Once the fine-tuning is completed, the adapter is merged into the pre-trained weights.

QLoRA [3] extends LoRA by quantizing the pretrained weights stored in GPU memory to reduce memory footprint.

$$\mathbf{W}_q = q(\mathbf{W}) \quad (2)$$

One difference between QLoRA and LoRA is that during fine-tuning, \mathbf{W}_q needs to be dequantized before involved into matrix multiplications:

$$\widetilde{\mathbf{W}} = \text{dq}(\mathbf{W}_q), \quad \mathbf{y} = \mathbf{x}(\widetilde{\mathbf{W}} + \mathbf{A}_k \mathbf{B}_k) \quad (3)$$

where $\text{dq}(\cdot)$ is the dequantization function. QLoRA introduces weight quantization error $(\mathbf{W} - \widetilde{\mathbf{W}})$, shifting the starting point of fine-tuning. To address this problem, LoftQ [1] initializes the adapter using the SVD-based low-rank approximation of $(\mathbf{W} - \widetilde{\mathbf{W}})$ to reduce the weight approximation error:

$$\arg \min_{\mathbf{A}_k, \mathbf{B}_k} \|\mathbf{W} - \widetilde{\mathbf{W}} - \mathbf{A}_k \mathbf{B}_k\|_F \quad (4)$$

Specifically, LoftQ uses a heuristic-based algorithm to iteratively update the quantized weights and the adapter (Algorithm 1 in the Appendix). Their experiments show that a larger number of iterations leads to a smaller weight error.

LQ-LoRA [3] also adopts LoftQ’s iterative method but keeps track of a scaled variant of the objective, $\arg \min_{\mathbf{A}_k, \mathbf{B}_k} \|\mathbf{D}_{\text{row}}(\mathbf{W} - \widetilde{\mathbf{W}} - \mathbf{A}_k \mathbf{B}_k) \mathbf{D}_{\text{col}}\|_F$, where \mathbf{D}_{row} and \mathbf{D}_{col} are heuristic homogenous row/column matrices from activation statistics. LQ-LoRA exits the iteration when the scaled objective function stops decreasing due to the lack of a theoretical justification for LoftQ.

b) *Quantization Error Reconstruction for PTQ*: Similar to the forward pass of fine-tuning in QLoRA, there are also PTQ methods that quantize the pretrained weights to low-precision formats and recover the model performance with additional low-rank terms. With a small enough rank k , the additional computation introduced is negligible. Note that unlike QPEFT which can utilize fine-tuning to correct the quantization error, PTQ methods aim to recover the model performance as much as possible without any training.

ZeroQuant-V2 [2] is the earliest weight-only quantization method introducing low-rank quantization error reconstruction to the PTQ problem. They apply SVD to the weight quantization error $(\mathbf{W} - \widetilde{\mathbf{W}})$ to calculate \mathbf{A}_k and \mathbf{B}_k (equivalent to LoftQ with one iteration). Combining low-rank terms and fine-grained quantization, ZeroQuant-V2 recovers the performance of 4-bit LLMs to a level comparable to 8-bit.

Recent quantization works have shown that activation statistics play a crucial role in weight-only LLM quantization [13, 10]. QLLM [9] trains the low-rank terms using gradient descent with a loss function that minimizes the output error of the attention layer. LQER [4] applies an activation-induced heuristic scale matrix \mathbf{S} to the quantization error before calculating SVD, $\mathbf{U}\Sigma\mathbf{V}^T = \text{SVD}(\mathbf{S}(\mathbf{W} - \widetilde{\mathbf{W}}))$, and assigns $\mathbf{A}_k := \mathbf{S}^{-1}\mathbf{U}_{:,k}$, $\mathbf{B}_k := \Sigma_{:k,:}\mathbf{V}_{:k,:}^T$. (Refer to Algorithm 2 in the Appendix). LQER achieves significant improvement over ZeroQuant-V2 and observes that in some layers singular values are shaped toward a more desirable distribution where singular values decay faster. Note that ZeroQuant-V2 can also be considered as a special case where \mathbf{S} in LQER is an identity matrix.

In summary, most of existing methods on QPEFT and PTQ target the minimization of the weight approximation error. Several recent works such as LQ-LoRA, QLLM, and LQER introduce activation-induced heuristics to the calculation of adapters/low-rank terms, but **a justification for the optimization objective and the corresponding analytical framework are still missing**.

III. OUR ANALYTICAL FRAMEWORK

In this section, we formulate the optimization objective of quantization error reconstruction and derive the analytical solution to the low-rank term $\mathbf{C}_k := \mathbf{A}_k\mathbf{B}_k$.

A. Problem Statement

Given a pretrained linear layer $\mathbf{y} = \mathbf{x}\mathbf{W}$ with input vector $\mathbf{x} \in \mathbb{R}^m$, output vector $\mathbf{y} \in \mathbb{R}^n$, and weight matrix $\mathbf{W} \in \mathbb{R}^{m \times n}$, our aim is to approximate it with a high-rank low-precision $\widetilde{\mathbf{W}}$ and a low-rank high-precision term $\mathbf{C}_k \in \mathbb{R}^{m \times n}$ with rank $k \ll \min(m, n)$.

$$\widetilde{\mathbf{y}} = \mathbf{x}(\widetilde{\mathbf{W}} + \mathbf{C}_k) \quad (5)$$

This raises the question of the actual optimization target: Should we minimize the weight reconstruction error $\|\mathbf{W} - \widetilde{\mathbf{W}}\|_F$ or the output reconstruction error $\|\mathbf{y} - \widetilde{\mathbf{y}}\|_2$? We separate these two problems and introduce them formally below.

Problem 1 (Minimization of weight error). For a pretrained linear layer $\mathbf{y} = \mathbf{x}\mathbf{W}$ and its approximated form $\widetilde{\mathbf{y}} = \mathbf{x}(\widetilde{\mathbf{W}} + \mathbf{C}_k)$, reconstructing the quantization error by minimizing weight approximation error has the following objective:

$$\arg \min_{\mathbf{C}_k} \|\mathbf{W} - \widetilde{\mathbf{W}} - \mathbf{C}_k\|_F \quad (6)$$

where $\|\cdot\|_F$ denotes the Frobenius norm.

Solution to Problem 1. From the Eckart-Young-Mirsky theorem [14], the optimal solution to Problem 1 with respect to rank k is the truncated SVD of the weight error matrix:

$$\mathbf{C}_k = \mathbf{U}_{:,k}\Sigma_{:k,:}\mathbf{V}_{:k,:}^T \quad (7)$$

where \mathbf{U} , Σ , and \mathbf{V}^T form the SVD of the weight quantization error, $\mathbf{U}\Sigma\mathbf{V}^T = \text{SVD}(\mathbf{W} - \widetilde{\mathbf{W}})$.

As noted in Section II, most existing works [1, 2, 3] in QPEFT and PTQ adopt this solution. However, we know that minimizing the weight approximation error is not equivalent to minimizing the layer output error. Furthermore, does minimizing the weight approximation error for each layer in a network effectively reduce the final model output error? We will show that the answer is negative in Section IV-B.

Problem 2 (Minimization of layer output error). For a pretrained linear layer $\mathbf{y} = \mathbf{x}\mathbf{W}$ and its approximated form $\widetilde{\mathbf{y}} = \mathbf{x}(\widetilde{\mathbf{W}} + \mathbf{C}_K)$, approximating the layer by minimizing the error between \mathbf{y} and $\widetilde{\mathbf{y}}$ is to minimize the following expectation.

$$\arg \min_{\mathbf{C}_k} \mathbb{E}_{\mathbf{y} \sim \mathbb{Y}} \{ \|\widetilde{\mathbf{y}} - \mathbf{y}\|_2^2 \} \quad (8)$$

where $\|\cdot\|_2$ denotes l_2 norm, and $\mathbb{Y} \subseteq \mathbb{R}^n$ is output space of the layer. We expand Equation (8) by substituting $\widetilde{\mathbf{y}}$ and \mathbf{y} :

$$\arg \min_{\mathbf{C}_k} \mathbb{E}_{\mathbf{x} \sim \mathbb{X}} \{ \|\mathbf{x}(\widetilde{\mathbf{W}} + \mathbf{C}_k) - \mathbf{x}\mathbf{W}\|_2^2 \} \quad (9)$$

where $\mathbb{X} \subseteq \mathbb{R}^m$ is the input space. In practice, the expectation can be approximated as a sample mean on a calibration dataset like a subset of the pretraining data set.

Problem 2 motivates some recent works [9, 3, 4] to involve activation-induced heuristics in the optimization of C_k . However, to our best knowledge, there is no work providing an analytical solution to this problem. In the following two sections, we will derive the analytical solution to Problem 2. More precisely, we present two solutions: one exact solution in Section III-B and an approximated solution based on a suitable statistical assumption in Section III-C.

B. QERA-exact: Analytical Solution

QERA-exact is our exact solution to Problem 2. QERA-exact is computationally expensive as it calculates the autocorrelation matrix of the input space \mathbb{X} . However, as we will show in Section IV, QERA-exact recovers significant model performance in extremely low-precision quantization.

Theorem 1 (QERA-exact solution). *The solution to Problem 2 is*

$$C_k = \left(\mathbf{R}_{\mathbb{X}\mathbb{X}}^{\frac{1}{2}} \right)^{-1} \mathbf{U}_{:,k} \boldsymbol{\Sigma}_{:k,:k} \mathbf{V}_{:k,:}^T \quad (10)$$

where $\mathbf{R}_{\mathbb{X}\mathbb{X}}$ is the autocorrelation matrix respect to the input space \mathbb{X} ,

$$\mathbf{R}_{\mathbb{X}\mathbb{X}} = \mathbb{E}_{\mathbf{x} \sim \mathbb{X}} \{ \mathbf{x}^T \mathbf{x} \} \quad (11)$$

$\mathbf{R}_{\mathbb{X}\mathbb{X}}^{\frac{1}{2}}$ represents the unique symmetric positive semi-definite matrix square root of $\mathbf{R}_{\mathbb{X}\mathbb{X}}$, and $\mathbf{U}_{:,k}$, $\boldsymbol{\Sigma}_{:k,:k}$, and $\mathbf{V}_{:k,:}$ form the truncated SVD of the following scaled weight error matrix,

$$\mathbf{U} \boldsymbol{\Sigma} \mathbf{V}^T = \text{SVD}(\mathbf{R}_{\mathbb{X}\mathbb{X}}^{\frac{1}{2}}(\mathbf{W} - \widetilde{\mathbf{W}})) \quad (12)$$

Remark 1. $\mathbf{R}_{\mathbb{X}\mathbb{X}}^{\frac{1}{2}}$ is positive semi-definite. In the event that it has a zero eigenvalue, it would be normal to add a small diagonal perturbation to recover invertibility. In practice, we ran extensive experiments and find that $\mathbf{R}_{\mathbb{X}\mathbb{X}}^{\frac{1}{2}}$ is invertible for all the pretrained models and datasets we present in Section IV.

Proof of Theorem 1

Proof. Define $\mathbf{P} := \widetilde{\mathbf{W}} + C_k - \mathbf{W}$, and $\mathbf{p}_i := \mathbf{P}_{i,:}$ is the i -th row of \mathbf{P} . Then we substitute $(\widetilde{\mathbf{W}} + C_k - \mathbf{W})$ in the expanded objective Equation (9) of Problem 2 with \mathbf{P} :

$$\begin{aligned} \mathbb{E}_{\mathbf{y} \sim \mathbb{Y}} \{ \|\widetilde{\mathbf{y}} - \mathbf{y}\|_2^2 \} &= \mathbb{E}_{\mathbf{x} \sim \mathbb{X}} \{ \|\mathbf{x}\mathbf{P}\|_2^2 \} \\ &= \mathbb{E}_{\mathbf{x} \sim \mathbb{X}} \{ \left\| \sum_{i=1}^m x_i \mathbf{p}_i \right\|_2^2 \} \\ &= \mathbb{E}_{\mathbf{x} \sim \mathbb{X}} \left\{ \sum_{i=1}^m \sum_{j=1}^m x_i x_j \mathbf{p}_i \mathbf{p}_j^T \right\} \end{aligned} \quad (13)$$

We rewrite the last line of Equation (13) as:

$$\mathbb{E}_{\mathbf{y} \sim \mathbb{Y}} \{ \|\widetilde{\mathbf{y}} - \mathbf{y}\|_2^2 \} = \mathbb{E}_{\mathbf{x} \sim \mathbb{X}} \{ \mathbf{e} \cdot ((\mathbf{x}^T \mathbf{x}) \odot (\mathbf{P} \mathbf{P}^T)) \cdot \mathbf{e}^T \} \quad (14)$$

where $\mathbf{e} = [1 \ 1 \ \dots \ 1]$ is a row vector of m ones, and \odot denotes the element-wise product.

Using the property of the element-wise product [15], the RHS of the above can be simplified.

$$\begin{aligned} \mathbb{E}_{\mathbf{y} \sim \mathbb{Y}} \{ \|\widetilde{\mathbf{y}} - \mathbf{y}\|_2^2 \} &= \mathbb{E}_{\mathbf{x} \sim \mathbb{X}} \{ \text{Tr} ((\mathbf{x}^T \mathbf{x})(\mathbf{P} \mathbf{P}^T)^T) \} \\ &= \text{Tr} (\mathbb{E}_{\mathbf{x} \sim \mathbb{X}} \{ \mathbf{x}^T \mathbf{x} \} \mathbf{P} \mathbf{P}^T) \\ &= \text{Tr} (\mathbf{R}_{\mathbb{X}\mathbb{X}} \mathbf{P} \mathbf{P}^T) \end{aligned} \quad (15)$$

where $\text{Tr}(\cdot)$ denotes trace and $\mathbf{R}_{\mathbb{X}\mathbb{X}} = \mathbb{E}_{\mathbf{x} \sim \mathbb{X}} \{ \mathbf{x}^T \mathbf{x} \}$ is the autocorrelation matrix with respect to the input space \mathbb{X} .

Since $\mathbf{R}_{\mathbb{X}\mathbb{X}}$ is a symmetric positive semi-definite matrix, it always has precisely one matrix square root, denoted as $\mathbf{R}_{\mathbb{X}\mathbb{X}}^{\frac{1}{2}}$, that is also symmetric and positive semi-definite [16]. We reorganize Equation (15) as the following since both $\mathbf{R}_{\mathbb{X}\mathbb{X}}$ and $(\mathbf{P} \mathbf{P}^T)$ are symmetric and positive semi-definite:

$$\begin{aligned} \mathbb{E}_{\mathbf{y} \sim \mathbb{Y}} \{ \|\widetilde{\mathbf{y}} - \mathbf{y}\|_2^2 \} &= \text{Tr} \left(\mathbf{R}_{\mathbb{X}\mathbb{X}}^{\frac{1}{2}} \mathbf{P} \mathbf{P}^T \mathbf{R}_{\mathbb{X}\mathbb{X}}^{\frac{1}{2}} \right) \\ &= \text{Tr} \left(\mathbf{R}_{\mathbb{X}\mathbb{X}}^{\frac{1}{2}} \mathbf{P} \mathbf{P}^T (\mathbf{R}_{\mathbb{X}\mathbb{X}}^{\frac{1}{2}})^T \right) \\ &= \|\mathbf{R}_{\mathbb{X}\mathbb{X}}^{\frac{1}{2}} \mathbf{P}\|_F^2 \end{aligned} \quad (16)$$

Now the objective of Problem 2 (Equation (8)) is equivalent to:

$$\begin{aligned} \arg \min_{C_k} \mathbb{E}_{y \sim \mathbb{Y}} \{ \| \tilde{y} - y \|^2_2 \} &= \arg \min_{C_k} \| R_{\mathbb{X} \mathbb{X}}^{\frac{1}{2}} P \|^2_F \\ &= \arg \min_{C_k} \| R_{\mathbb{X} \mathbb{X}}^{\frac{1}{2}} (\tilde{W} + C_k - W) \|^2_F \end{aligned} \quad (17)$$

If we assign $Q := R_{\mathbb{X} \mathbb{X}}^{\frac{1}{2}} (W - \tilde{W})$ and $Q_k := R_{\mathbb{X} \mathbb{X}}^{\frac{1}{2}} C_k$, the objective becomes:

$$\arg \min_Q \| Q_k - Q \|^2_F \quad (18)$$

Note that multiplication by the invertible matrix $R_{\mathbb{X} \mathbb{X}}^{\frac{1}{2}}$ (Remark 1) does not change the rank of the matrix C_k . According to the Eckart-Young-Mirsky theorem [14], the optimal rank k approximation to Q_k is the truncated SVD of Q :

$$Q_k = U_{:,k} \Sigma_{:k,:k} V_{:k,:}^T \quad (19)$$

where $U \Sigma V^T = \text{SVD}(Q) = \text{SVD}\left(R_{\mathbb{X} \mathbb{X}}^{\frac{1}{2}} (W - \tilde{W})\right)$. Thus the optimal rank- k solution to C_k is:

$$C_k = \left(R_{\mathbb{X} \mathbb{X}}^{\frac{1}{2}}\right)^{-1} Q_k = \left(R_{\mathbb{X} \mathbb{X}}^{\frac{1}{2}}\right)^{-1} U_{:,k} \Sigma_{:k,:k} V_{:k,:}^T \quad (20)$$

□

In practice, we assign $A_k := \left(R_{\mathbb{X} \mathbb{X}}^{\frac{1}{2}}\right)^{-1} U_{:,k}$ and $B_k := \Sigma_{:k,:k} V_{:k,:}^T$. Note that QERA adds no constraints to the quantization (and dequantization) function $q(\cdot)$ (and $dq(\cdot)$), *i.e.*, the low-precision \tilde{W} can be obtained by any quantization method.

C. QERA-approx: An Analytical Solution with the Uncorrelated Assumption

QERA-approx is our analytical solution to Problem 2 based on the assumption that different embedding dimensions are uncorrelated. This solution is more computationally efficient than the exact solution, and the assumption is testable on real-world datasets. The complete proof of QERA-approx is in Appendix B.

Assumption 1. For a pretrained linear layer $y = xW$, the expectation of the product of different embedding dimensions is zero:

$$\mathbb{E}_{x \sim \mathbb{X}} \{ x_i x_j \} = 0, \quad \forall i \neq j \quad (21)$$

where x_i and x_j are the i -th and j -th elements of the input vector x .

We test this assumption on LLMs in Section V.

Theorem 2 (QERA-approx solution). *The solution to Problem 2 based on Assumption 1 is:*

$$C_k = S^{-1} U_{:,k} \Sigma_{:k,:k} V_{:k,:}^T \quad (22)$$

where S is a diagonal matrix built from activation statistics,

$$S = \text{diag}(\sqrt{\mathbb{E}_{x \sim \mathbb{X}} \{ x_1^2 \}}, \sqrt{\mathbb{E}_{x \sim \mathbb{X}} \{ x_2^2 \}}, \dots, \sqrt{\mathbb{E}_{x \sim \mathbb{X}} \{ x_m^2 \}}) \quad (23)$$

and U , Σ , V^T form the SVD of the following scaled weight error matrix,

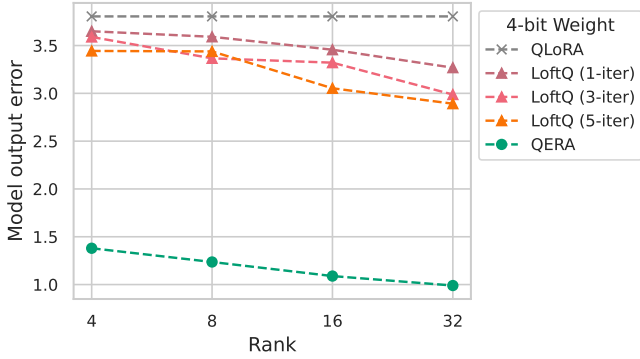
$$U \Sigma V^T = \text{SVD}(S(W - \tilde{W})) \quad (24)$$

Remark 2. For the diagonal matrix S in Theorem 2 to be invertible, we need $\mathbb{E}_{x \sim \mathbb{X}} \{ x_i^2 \} \neq 0$ for all dimension i . In practice, this is almost always true for pretrained layers because no dimension in the input embeddings is always zero.

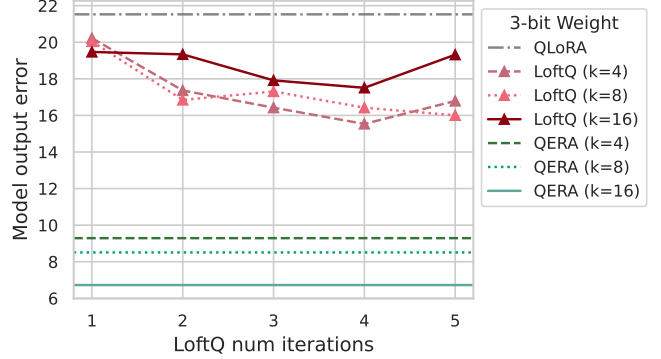
For implementation, we assign $A_k := S^{-1} U_{:,k}$ and $B_k := \Sigma_{:k,:k} V_{:k,:}$ to form the low-rank terms to save the memory and computation cost. Interestingly, QERA-approx solution is similar to the activation-induced heuristics in LQER [4], which calibrates the average absolute value on the embedding dimension (Refer to Algorithm 2 in the Appendix). In Section IV-C, we will show that our solution is more effective in practice and resolves the discrepancy between the recovered model performance and the number of calibration samples in LQER.

IV. EXPERIMENTS

In this section, we first introduce the experiment setup in Section IV-A. Then we present the results of our experiments on QPEFT and PTQ in Section IV-B and Section IV-C respectively.



(a) Model output error vs. rank



(b) Model output error vs. LoftQ iterations

Fig. 1: The model output error of RoBERTa-base before fine-tuning. We feed 128 samples from RoBERTa’s pretraining dataset and profile the output logits error between the adapted and the FP32 model. We sweep the rank k and the iteration number of LoftQ on 4-bit and 3-bit models. In LoftQ, neither more iterations nor a higher rank guarantees lower model output error, though the weight approximation error of every layer decreases. In contrast, QERA-approx consistently has the lowest model output error across all settings, and the error monotonically decreases as the rank increases.

A. Experiment Setup

We perform fine-tuning and quantization experiments separately, and compare with their respective SoTA methods. The experiments take around 6400 GPU hours in total. The hardware platform, separate GPU hours, software dependencies, and random seed settings can be found in Appendix C.

For fine-tuning experiments, we use Theorem 2, noted as QERA-approx, to initialize low-rank terms, and compare with full-finetuning, LoRA [12], QLoRA [17], and LoftQ [1]. Specifically, we adopt 5-iteration LoftQ, which is the officially recommended setup. We include both encoder-only model experiments (fine-tuning RoBERTa-base [18] on GLUE [19]) and decoder-only LLM experiments (fine-tuning LLaMA-2 [20] and LLaMA-3.1 [7] on continuous pretraining task SlimPajama [21] and supervised fine-tuning task GSM8K [22]). For each method/baseline, we sweep the learning rate and record the best result. The final results are averaged over three random seeds. The learning rate ranges and batch sizes are listed in Appendix C1.

For quantization experiments, we use both Theorem 1, noted as QERA-exact, and Theorem 2 (QERA-approx) to calculate the low-rank error reconstruction terms and report results separately. We compare with BF16, quantized model without error reconstruction terms (w -only), ZeroQuant-V2 [2], and LQER [4] at different precision setups. We also include HQQ [23], a leading 4-bit method that does not use quantization error reconstruction. We quantize LLMs of various sizes and model family, including TinyLlama [24], Gemma-2 [25], Phi-3.5 [26] and LLaMA-2/-3.1 [20, 7]. We use lm-evaluation-harness to report results on Wikitext2 [27], ARC (challenge) [28], BoolQ [29], CommonsenseQA [30], Winogrande [31], MMLU [32], and BigBench-Hard [33]. We also evaluate instruction-tuned model, Vicuna-v1.5 [34], with AlpacaEval 2.0 [35], which is an automatic evaluation tool for instruction-following tasks. Detailed setup is in Appendix C2.

B. Improved QPEFT

We first identify a pitfall in the commonly-used iterative Algorithm 1, that is, minimizing the weight approximation error for each layer does not necessarily minimize the model output error. Then we show that our QERA initialization enables a clear reduction in the model output error at the start of fine-tuning, leading to better fine-tuned accuracy/perplexity and faster convergence.

a) *Reduced layer weight error \neq reduced model output error*: We apply 4-bit and 3-bit QLoRA, LoftQ, and QERA-approx to RoBERTa-base and inspect the *model output error* on RoBERTa’s pretraining dataset before fine-tuning at rank $k = 4, 8, 16, 32$. For LoftQ, we also sweep the number of iterations from 1 to 5. In Figure 1, we observe that

- For LoftQ, given a specific rank, increasing the optimization iterations does not guarantee a reduced model output error. Though all the layers’ weight approximation errors monotonically decrease with the number of iterations (as illustrated in Figure 6 in Appendix), the model output error does not monotonically decrease. For example, in Figure 1a, the model output error of LoftQ (5-iter) is larger than LoftQ (3-iter) at rank $k = 8$.
- For LoftQ, given a specific number of iterations, increasing the rank does not guarantee a reduced model output error. For example, in Figure 1b, the output error of LoftQ (rank $k = 16$) is larger than LoftQ (rank $k = 4$) and $k = 8$ at 2, 3, 4, and 5 iterations.

TABLE I: Fine-tuning results of RoBERTa-base on GLUE. QERA-approx outperforms LoftQ across all bit widths, and the improvement is more obvious with aggressive quantization. QERA achieves $\Delta_{\text{acc}} = 4.12\%$ higher than LoftQ at 3-bit and 6.05% at 2-bit.

Rank	W-bits	Method	MNLI Acc	QNLI Acc	RTE Acc	SST Acc	MRPC Acc	CoLA Matt	QQP Acc	STSB P/S Corr	Avg.
-	16	Full FT	87.61	92.95	73.16	94.88	92.15	60.41	91.61	90.44/90.25	85.38
8	16	LoRA	87.85	92.84	69.55	94.46	89.99	57.52	89.83	89.92/89.83	84.00
8	4.25	QLoRA	87.21	92.32	63.90	94.08	88.24	56.08	90.55	89.59/89.56	82.75
		LoftQ (5-iter)	87.27	92.48	67.13	94.38	88.24	54.59	90.51	88.75/88.79	82.92
		QERA-approx	87.28	92.45	70.40	94.38	88.97	55.99	90.39	89.83/89.72	83.71
8	3.25	QLoRA	84.87	89.58	53.67	91.02	73.94	3.12	89.31	84.80/84.38	71.29
		LoftQ (5-iter)	85.24	89.65	58.24	92.05	75.82	11.00	88.93	85.55/85.27	73.31
		QERA-approx	85.58	90.74	58.48	92.59	82.19	32.98	89.41	87.43/87.08	77.43
64	2.50	QLoRA	77.87	85.26	54.15	90.02	71.00	0	87.93	74.72/75.31	67.62
		LoftQ (5-iter)	80.15	87.65	52.95	90.94	74.35	3.43	89.17	82.76/82.90	70.18
		QERA-exact	84.64	90.05	58.48	92.32	84.72	26.43	89.69	86.48/86.40	76.23

TABLE II: Fine-tuning results of LLaMA-2-7B and LLaMA-3.1-8B on SlimPajama and GSM8K. A trend similar to RoBERTa experiments are observed, *i.e.*, QERA outperforms QLoRA and LoftQ and the improvement is more obvious on aggressive quantization.

W-bits	Method	LLaMA-2-7B		LLaMA-3.1-8B	
		SlimPajama (Δ_{ppl})	GSM8K (Δ_{acc})	SlimPajama (Δ_{ppl})	GSM8K (Δ_{acc})
16	LoRA	6.17	39.40	8.07	55.72
4.25	QLoRA	6.44 (+0.27)	30.71 (-8.69)	8.70 (+0.63)	54.81 (-0.91)
	LoftQ (5-iter)	6.39 (+0.22)	28.58 (-10.82)	8.73 (+0.66)	54.23 (-1.49)
	QERA-approx	6.33 (+0.16)	32.26 (-7.14)	8.68 (+0.61)	55.24 (-0.48)
2.25	QLoRA	53.95 (+47.78)	12.79 (-18.31)	71.90 (+63.83)	5.08 (-50.64)
	LoftQ (5-iter)	12.30 (+6.13)	18.37 (-12.73)	27.16 (+19.09)	13.72 (-42.00)
	QERA-approx	10.56 (+4.39)	18.78 (-12.32)	20.07 (+12.00)	19.41 (-36.31)

- The model output error of our QERA-approx is always smaller than LoftQ and QLoRA, across all precision and rank settings. Moreover, the output error of QERA-approx monotonically decreases as the rank increases.

This empirical evidence suggests a strong correlation between the reduction of layer output error and the decrease in model output error. Conversely, minimizing weight approximation error does not demonstrate a comparable impact on overall model performance.

b) Better optimization quality: Table I and Table II summarize the fine-tuning experiments of RoBERTa-base on GLUE, and LLaMA-2-7B/3.1-8B fine-tuned on SlimPajama and GSM8K, respectively. QERA outperforms both LoftQ and QLoRA. In GLUE experiments, at 4-bit, QERA enables an average accuracy gain of 0.96% and 0.79% higher than QLoRA and LoftQ respectively, close to BF16 LoRA; At 3-bit and 2-bit, QERA achieves a 4.12% and 6.05% higher average accuracy than LoftQ respectively. Similar trends are observed on LLM fine-tuning experiments, *i.e.*, QERA outperforms QLoRA and LoftQ, and the advantage of QERA over LoftQ is more obvious with more aggressive quantization.

c) Faster Convergence: QERA initialization also speeds up the training convergence. For LLM fine-tuning, this is expected as QERA initialization is closer to the full-precision model. Interestingly, in encoder-only experiments

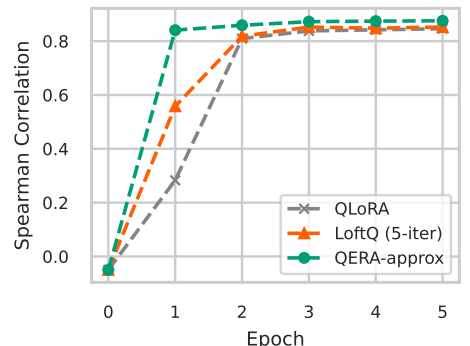


Fig. 2: Faster convergence of QERA-approx on STSB.

TABLE III: Perplexity (\downarrow) of LLMs on WikiText2. w -only denotes the quantized model without low-rank error reconstruction. QERA-approx outperforms LQER on almost all setups and QERA-exact achieves the lowest perplexity. The advantage of QERA is pronounced at 3-bit.

W-bits	Method	Rank	TinyLlama	Gemma-2	Phi-3.5	LLaMA-2		LLaMA-3.1	
			1.1B	2B	3.8B	7B	13B	8B	80B
-	BF16	-	13.98	13.08	11.50	8.71	7.68	7.55	3.06
4.25	HQQ	-	15.02	14.29	14.63	9.59	8.27	8.72	3.97
4.25	w -only	32	19.40	16.23	14.16	9.45	8.06	8.78	4.55
	ZeroQuant-V2		18.03	15.71	14.09	9.42	8.07	8.83	4.48
	LQER		16.23	14.55	12.88	9.22	7.96	8.45	4.10
	QERA-approx		15.66	14.60	12.81	9.17	7.95	8.45	4.10
3.25	QERA-exact	64	16.16	14.12	12.30	9.12	7.93	8.33	3.82
	w -only		32.82	41.13	47.78	13.32	10.24	18.96	16.46
	ZeroQuant-V2		27.80	33.56	42.64	13.00	10.03	19.29	10.12
	LQER		20.60	21.99	18.27	14.00	9.09	11.86	7.05
	QERA-approx		20.43	21.93	17.99	10.99	9.04	11.73	6.99
	QERA-exact		19.51	19.97	20.37	10.67	8.97	11.39	6.68

on GLUE where the model classifier head is randomly initialized, we also observe that QERA converges faster, especially on small subsets such as STSB and MRPC where only a few thousand samples are available (in comparison MNLI has 393k samples and QQP has 364k samples). For example, in Figure 2, the Spearman correlation coefficient of QERA on STSB increases and converges faster than LoftQ and QLoRA, as the green line plateaus first.

C. Improved PTQ

In this part, we first demonstrate that LQER, which depends on heuristics derived from activation values, does not guarantee improved performance with a larger calibration dataset. However, QERA exhibits the opposite trend. Through extensive experiments, we show that QERA consistently outperforms ZeroQuant-V2 and LQER, and QERA-exact exhibits better model performance than QERA-approx at the cost of more computation in the quantization process. These results verified the effectiveness of our analytical solution.

a) *Model performance vs. calibration set size.*: As mentioned at the end of Section III-C, the scale matrix in LQER [4] is similar to the one in QERA-approx, but is based on hand-crafted heuristics. As a result, we observe that the model performance of LQER varies randomly as the number of calibration samples increases (the purple curve in Figure 3). On the contrary, more calibration samples consistently lead to better model performance for QERA until convergence.

b) *Improved perplexity and downstream task accuracy*: We apply QERA-approx and QERA-exact to a range of models and evaluate on both pretraining task and downstream tasks in Table III and Table IV respectively. We also compare to HQQ, a SoTA method that does not use quantization error reconstruction.

On most models, QERA-approx outperforms ZeroQuant-V2 and LQER, while QERA-exact achieves the best performance. At 4-bit, QERA-exact is nearly lossless. At 3-bit, QERA-exact’s improvement over QERA-approx (Table III) is clear, indicating the superiority of QERA-exact for aggressive quantization.

c) *Higher win rate on AlpacaEval 2.0*: To better understand the impact on instruction-tuned models, we present the results of Vicuna-7b-v1.5 on AlpacaEval 2.0. In Figure 4, we evaluate the quantization-error-reconstruction-based methods against the w -only quantization counterpart. QERA outperforms ZeroQuant-V2 and LQER by a higher win rate, indicating a better response quality.

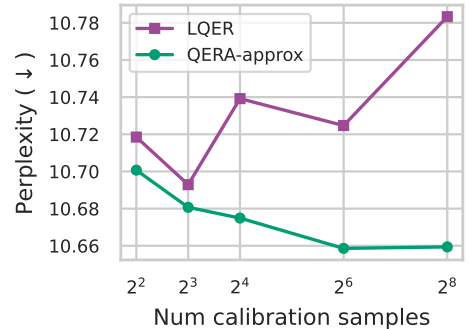


Fig. 3: QERA resolves the discrepancy between the recovered model performance and the number of calibration samples in LQER.

¹The average accuracy of TinyLlama-1.1B excludes BoolQ, CommonsenseQA, and MMLU since TinyLlama-1.1B has random guess accuracy on these tasks.

TABLE IV: Average accuracy (\uparrow) of LLMs on six downstream tasks. QERA-exact outperforms other quantization-error reconstruction-based methods across almost all models. We also compare to HQQ [23], a SoTA PTQ method that does not adopt quantization-error reconstruction or activation heuristics. QERA-exact achieves an average accuracy on par with HQQ.

W-bits	Method	Rank	TinyLlama ¹	Gemma-2	Phi-3.5	LLaMA-2	LLaMA-3.1		
			1.1B	2B	3.8B	7B	13B	8B	80B
-	BF16	-	40.59	53.96	66.91	49.61	55.74	63.88	72.05
4.25	HQQ	-	40.35	52.54	59.17	48.26	54.53	62.59	71.31
4.25	<i>w</i> -only	-	36.56	48.33	64.52	47.62	55.12	61.53	68.46
	ZeroQuant-V2		37.26	48.24	64.44	47.43	55.15	61.70	68.45
	LQER	32	40.45	49.77	64.46	48.47	55.40	61.75	70.94
	QERA-approx		40.02	49.29	64.53	48.52	55.20	61.68	70.80
	QERA-exact		40.36	51.73	65.08	48.91	55.42	62.05	71.42

V. DISCUSSION

In this section, we revisit the arguments, design choices, and observations made in the previous sections, including a test of Assumption 1, and the choice of the calibration set for PEFT. An extended discussion of numeric stability and scalability of QERA is in Appendix G, and LoRA rank and model choices of PEFT experiments is in Appendix H.

a) *Test of Assumption 1*: To test Assumption 1, we profile the autocorrelation matrix $\mathbf{R}_{\mathbf{XX}}$ of the linear layer inputs in LLaMA-2-7B and LLaMA-3-8B. Note that $\mathbb{E}_{\mathbf{x} \sim \mathbf{X}}\{\mathbf{x}_i \mathbf{x}_j\}$, which assumes to be zero for $i \neq j$ in Assumption 1. Figure 5 shows the normalized $\mathbb{E}_{\mathbf{x} \sim \mathbf{X}}\{\mathbf{x}_i \mathbf{x}_j\}$, of four representative layers in LLaMA-3-8B where darker elements denote values closer to zero. There are several layers with some input dimensions strongly correlated with others, such as the inputs to the third attention layer in Figure 5a, but for most layers, our assumption holds, especially the MLP layers, such as Figures 5b to 5d. More $\mathbb{E}_{\mathbf{x} \sim \mathbf{X}}\{\mathbf{x}_i \mathbf{x}_j\}$ plots are in Appendix E.

b) *Choice of calibration set for QPEFT*: One problem is to determine the calibration set for QERA before fine-tuning. In 2-bit RoBERTa-base fine-tuning experiment on SST2 (Appendix F), we find that calibrating on the pretraining dataset, WikiText2, helps the loss to decrease. However, the loss of the model calibrated on the fine-tuning dataset does not follow the same trend. We hypothesize that the massive padding tokens in preprocessed SST2 samples cause this discrepancy, especially considering that the sequence length of the raw SST2 dataset changes fiercely.

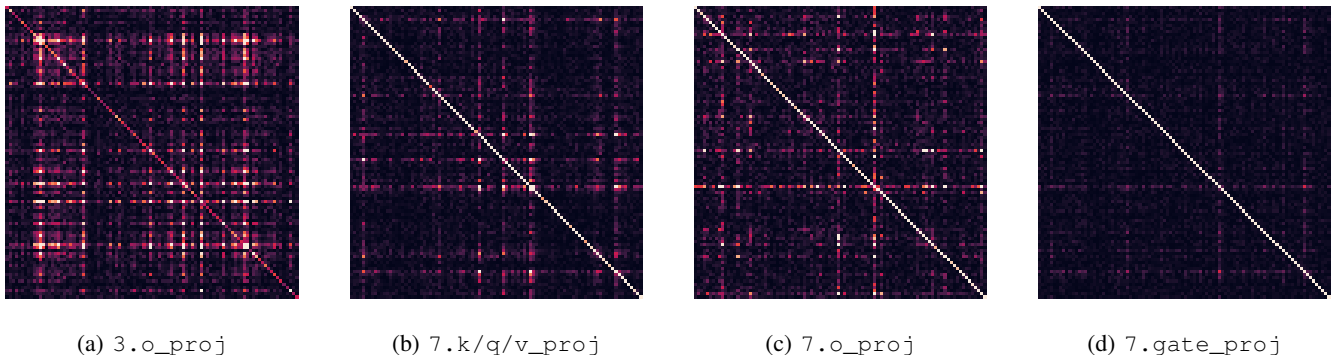


Fig. 5: Normalized $\text{abs}(\mathbf{R}_{\mathbf{XX}})$ of the layer inputs in LLaMA-3-8B. Dark elements denotes value close to zero. There are a few layers with input dimensions strongly correlated with others, such as the third attention layer in (a), but for most layers, our assumption of zero-expectation holds.

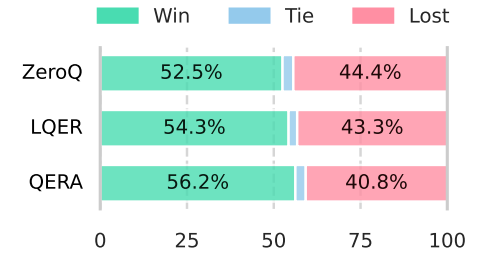


Fig. 4: AlpacaEval 2.0 evaluation results. We compare quantized models to the counterpart without quantization-error reconstruction. A higher **win rate** (\uparrow) indicates better instruction-following performance.

VI. CONCLUSION

In this paper, we formulate the problem of quantization error reconstruction and propose QERA as an analytical solution. Applying QERA to related works for efficient fine-tuning or inference, we show that QERA resolves the discrepancy in existing methods, and outperforms SoTA methods in both fine-tuning and quantization tasks by a clear margin.

REFERENCES

- [1] Y. Li, Y. Yu, C. Liang, P. He, N. Karampatziakis, W. Chen, and T. Zhao, “Loftq: Lora-fine-tuning-aware quantization for large language models,” *arXiv preprint arXiv:2310.08659*, 2023.
- [2] Z. Yao, X. Wu, C. Li, S. Youn, and Y. He, “Zeroquant-v2: Exploring post-training quantization in llms from comprehensive study to low rank compensation,” *arXiv preprint arXiv:2303.08302*, 2023.
- [3] H. Guo, P. Greengard, E. P. Xing, and Y. Kim, “Lq-lora: Low-rank plus quantized matrix decomposition for efficient language model finetuning,” *arXiv preprint arXiv:2311.12023*, 2023.
- [4] C. Zhang, J. Cheng, G. A. Constantinides, and Y. Zhao, “Lqer: Low-rank quantization error reconstruction for llms,” *arXiv preprint arXiv:2402.02446*, 2024.
- [5] A. Faiz, S. Kaneda, R. Wang, R. Osi, P. Sharma, F. Chen, and L. Jiang, “Llmcarbon: Modeling the end-to-end carbon footprint of large language models,” *arXiv preprint arXiv:2309.14393*, 2023.
- [6] J. Kaplan, S. McCandlish, T. Henighan, T. B. Brown, B. Chess, R. Child, S. Gray, A. Radford, J. Wu, and D. Amodei, “Scaling laws for neural language models,” *arXiv preprint arXiv:2001.08361*, 2020.
- [7] A. Dubey, A. Jauhri, A. Pandey, A. Kadian, A. Al-Dahle, A. Letman, A. Mathur, A. Schelten, A. Yang, A. Fan *et al.*, “The llama 3 herd of models,” *arXiv preprint arXiv:2407.21783*, 2024.
- [8] N. Ding, Y. Qin, G. Yang, F. Wei, Z. Yang, Y. Su, S. Hu, Y. Chen, C.-M. Chan, W. Chen *et al.*, “Parameter-efficient fine-tuning of large-scale pre-trained language models,” *Nature Machine Intelligence*, vol. 5, no. 3, pp. 220–235, 2023.
- [9] J. Liu, R. Gong, X. Wei, Z. Dong, J. Cai, and B. Zhuang, “Qllm: Accurate and efficient low-bitwidth quantization for large language models,” *arXiv preprint arXiv:2310.08041*, 2023.
- [10] J. Lin, J. Tang, H. Tang, S. Yang, W.-M. Chen, W.-C. Wang, G. Xiao, X. Dang, C. Gan, and S. Han, “Awq: Activation-aware weight quantization for on-device llm compression and acceleration,” *Proceedings of Machine Learning and Systems*, vol. 6, pp. 87–100, 2024.
- [11] W. Shao, M. Chen, Z. Zhang, P. Xu, L. Zhao, Z. Li, K. Zhang, P. Gao, Y. Qiao, and P. Luo, “Omniquant: Omnidirectionally calibrated quantization for large language models,” *arXiv preprint arXiv:2308.13137*, 2023.
- [12] E. J. Hu, Y. Shen, P. Wallis, Z. Allen-Zhu, Y. Li, S. Wang, L. Wang, and W. Chen, “Lora: Low-rank adaptation of large language models,” *arXiv preprint arXiv:2106.09685*, 2021.
- [13] Z. Liu, B. Oguz, C. Zhao, E. Chang, P. Stock, Y. Mehdad, Y. Shi, R. Krishnamoorthi, and V. Chandra, “Llm-qat: Data-free quantization aware training for large language models,” *arXiv preprint arXiv:2305.17888*, 2023.
- [14] C. Eckart and G. Young, “The approximation of one matrix by another of lower rank,” *Psychometrika*, vol. 1, no. 3, pp. 211–218, 1936.
- [15] G. P. Styan, “Hadamard products and multivariate statistical analysis,” *Linear algebra and its applications*, vol. 6, pp. 217–240, 1973.
- [16] R. A. Horn and C. R. Johnson, *Matrix analysis*. Cambridge university press, 2012.
- [17] T. Dettmers, A. Pagnoni, A. Holtzman, and L. Zettlemoyer, “Qlora: Efficient finetuning of quantized llms,” *Advances in Neural Information Processing Systems*, vol. 36, 2024.
- [18] Y. Liu, “Roberta: A robustly optimized bert pretraining approach,” *arXiv preprint arXiv:1907.11692*, 2019.
- [19] Z.-X. Ye, Q. Chen, W. Wang, and Z.-H. Ling, “Align, mask and select: A simple method for incorporating commonsense knowledge into language representation models,” *arXiv preprint arXiv:1908.06725*, 2019.
- [20] H. Touvron, L. Martin, K. Stone, P. Albert, A. Almahairi, Y. Babaei, N. Bashlykov, S. Batra, P. Bhargava, S. Bhosale *et al.*, “Llama 2: Open foundation and fine-tuned chat models,” *arXiv preprint arXiv:2307.09288*, 2023.
- [21] D. Soboleva, F. Al-Khateeb, R. Myers, J. R. Steeves, J. Hestness, and N. Dey, “SlimPajama: A 627B token cleaned and deduplicated version of RedPajama,” <https://www.cerebras.net/blog/slimpajama-a-627b-token-cleaned-and-deduplicated-version-of-redpajama>, 2023. [Online]. Available: <https://huggingface.co/datasets/cerebras/SlimPajama-627B>
- [22] K. Cobbe, V. Kosaraju, M. Bavarian, M. Chen, H. Jun, L. Kaiser, M. Plappert, J. Tworek, J. Hilton, R. Nakano, C. Hesse, and J. Schulman, “Training verifiers to solve math word problems,” *arXiv preprint arXiv:2110.14168*, 2021.
- [23] H. Badri and A. Shaji, “Half-quadratic quantization of large machine learning models,” November 2023. [Online]. Available: https://mobiusml.github.io/hqq_blog/
- [24] P. Zhang, G. Zeng, T. Wang, and W. Lu, “Tinyllama: An open-source small language model,” 2024.
- [25] G. Team, M. Riviere, S. Pathak, P. G. Sessa, C. Hardin, S. Bhupatiraju, L. Hussenot, T. Mesnard, B. Shahriari, A. Ramé *et al.*, “Gemma 2: Improving open language models at a practical size,” *arXiv preprint arXiv:2408.00118*, 2024.

- [26] M. Abdin, S. A. Jacobs, A. A. Awan, J. Aneja, A. Awadallah, H. Awadalla, N. Bach, A. Bahree, A. Bakhtiari, H. Behl *et al.*, “Phi-3 technical report: A highly capable language model locally on your phone,” *arXiv preprint arXiv:2404.14219*, 2024.
- [27] S. Merity, C. Xiong, J. Bradbury, and R. Socher, “Pointer sentinel mixture models,” 2016.
- [28] P. Clark, I. Cowhey, O. Etzioni, T. Khot, A. Sabharwal, C. Schoenick, and O. Tafjord, “Think you have solved question answering? try arc, the ai2 reasoning challenge,” *arXiv:1803.05457v1*, 2018.
- [29] C. Clark, K. Lee, M.-W. Chang, T. Kwiatkowski, M. Collins, and K. Toutanova, “Boolq: Exploring the surprising difficulty of natural yes/no questions,” *arXiv preprint arXiv:1905.10044*, 2019.
- [30] A. Talmor, J. Herzig, N. Lourie, and J. Berant, “CommonsenseQA: A question answering challenge targeting commonsense knowledge,” in *Proceedings of the 2019 Conference of the North American Chapter of the Association for Computational Linguistics: Human Language Technologies, Volume 1 (Long and Short Papers)*. Minneapolis, Minnesota: Association for Computational Linguistics, Jun. 2019, pp. 4149–4158. [Online]. Available: <https://aclanthology.org/N19-1421>
- [31] K. Sakaguchi, R. Le Bras, C. Bhagavatula, and Y. Choi, “An adversarial winograd schema challenge at scale,” *arXiv preprint arXiv:1907.10641*, 2019.
- [32] D. Hendrycks, C. Burns, S. Basart, A. Zou, M. Mazeika, D. Song, and J. Steinhardt, “Measuring massive multitask language understanding,” *Proceedings of the International Conference on Learning Representations (ICLR)*, 2021.
- [33] M. Suzgun, N. Scales, N. Schärli, S. Gehrmann, Y. Tay, H. W. Chung, A. Chowdhery, Q. V. Le, E. H. Chi, D. Zhou, , and J. Wei, “Challenging big-bench tasks and whether chain-of-thought can solve them,” *arXiv preprint arXiv:2210.09261*, 2022.
- [34] L. Zheng, W.-L. Chiang, Y. Sheng, S. Zhuang, Z. Wu, Y. Zhuang, Z. Lin, Z. Li, D. Li, E. Xing *et al.*, “Judging llm-as-a-judge with mt-bench and chatbot arena,” *Advances in Neural Information Processing Systems*, vol. 36, pp. 46595–46623, 2023.
- [35] Y. Dubois, B. Galambosi, P. Liang, and T. B. Hashimoto, “Length-controlled alpacaeval: A simple way to debias automatic evaluators,” *arXiv preprint arXiv:2404.04475*, 2024.
- [36] E. Deadman, N. J. Higham, and R. Ralha, “Blocked schur algorithms for computing the matrix square root,” in *International Workshop on Applied Parallel Computing*. Springer, 2012, pp. 171–182.
- [37] B. Darvish Rouhani, R. Zhao, V. Elango, R. Shafipour, M. Hall, M. Mesmakhosroshahi, A. More, L. Melnick, M. Golub, G. Varatkar *et al.*, “With shared microexponents, a little shifting goes a long way,” in *Proceedings of the 50th Annual International Symposium on Computer Architecture*, 2023, pp. 1–13.
- [38] F. Meng, Z. Wang, and M. Zhang, “Pissa: Principal singular values and singular vectors adaptation of large language models,” *arXiv preprint arXiv:2404.02948*, 2024.
- [39] J. Chee, Y. Cai, V. Kuleshov, and C. M. De Sa, “Quip: 2-bit quantization of large language models with guarantees,” *Advances in Neural Information Processing Systems*, vol. 36, 2024.
- [40] P. He, J. Gao, and W. Chen, “Debertav3: Improving deberta using electra-style pre-training with gradient-disentangled embedding sharing,” *arXiv preprint arXiv:2111.09543*, 2021.
- [41] Q. Zhang, M. Chen, A. Bukharin, N. Karampatziakis, P. He, Y. Cheng, W. Chen, and T. Zhao, “Adalora: Adaptive budget allocation for parameter-efficient fine-tuning,” *arXiv preprint arXiv:2303.10512*, 2023.

APPENDIX

A. Algorithms in Related Work

Here we summarize the algorithm of LoftQ [1] in Algorithm 1 and LQER [4] in Algorithm 2 respectively. LQ-LoRA [3] adopts a variant of Algorithm 1. ZeroQuant-V2 [2] can be considered as Algorithm 1 with one iteration, or a special case of Algorithm 2 where the scale matrix \mathbf{S} is an identity matrix.

Algorithm 1 LoftQ [1]

Require: Pretrained weight \mathbf{W} , target rank k , quantization function $q(\cdot)$, dequantization function $dq(\cdot)$, number of iterations T

- 1: $\mathbf{A}_k \leftarrow \mathbf{0}$, $\mathbf{B}_k \leftarrow \mathbf{0}$
- 2: **for** $i = 1$ to T **do**
- 3: $\mathbf{W}_q \leftarrow q(\mathbf{W} - \mathbf{A}_k \mathbf{B}_k)$ {Update quantized weight matrix}
- 4: $\widetilde{\mathbf{W}} \leftarrow dq(\mathbf{W}_q)$
- 5: $\mathbf{U}, \Sigma, \mathbf{V}^T \leftarrow \text{SVD}(\mathbf{W} - \widetilde{\mathbf{W}})$ {SVD-based rank- k approximation}
- 6: $\mathbf{A}_k \leftarrow \mathbf{U}_{:,k} \sqrt{\Sigma_{:,k}}, \mathbf{B}_k \leftarrow \sqrt{\Sigma_{:,k}} \mathbf{V}_{:,k}^T$
- 7: **end for**

Algorithm 2 LQER [4]

Require: Pretrained weight \mathbf{W} , target rank k , quantization function $q(\cdot)$, dequantization function $dq(\cdot)$, calibration dataset $\mathbb{X} = \{\mathbf{x}_i \in \mathbb{R}^m | i = 1, \dots, N\}$

- 1: Initialize vector $\mathbf{s} \leftarrow \mathbf{0}$
- 2: **for** sample \mathbf{x} in \mathbb{X} **do**
- 3: $\mathbf{s} \leftarrow \mathbf{s} + \text{abs}(\mathbf{x})$ {Calibrate by accumulating activation magnitude on each dimension}
- 4: **end for**
- 5: $\mathbf{S} \leftarrow \frac{1}{N} \text{diag}(\mathbf{s})$ {Construct a diagonal matrix \mathbf{S} }
- 6: $\mathbf{W}_q \leftarrow q(\mathbf{W})$
- 7: $\widetilde{\mathbf{W}} \leftarrow dq(\mathbf{W}_q)$
- 8: $\mathbf{U}, \Sigma, \mathbf{V}^T \leftarrow \text{SVD}(\mathbf{S}(\mathbf{W} - \widetilde{\mathbf{W}}))$ {SVD on the scaled weight error}
- 9: $\mathbf{A}_k \leftarrow \mathbf{S}^{-1} \mathbf{U}_{:,k}, \mathbf{B}_k \leftarrow \Sigma_{:,k} \mathbf{V}_{:,k}^T$ {Rank- k approximation with un-scaling}

B. Proof of Theorem 2

Here we present the full proof of QERA-approx. QERA-approx is an approximated solution to Problem 2 based on Assumption 1, which is suitable to initialize the low-rank terms in fine-tuning for lower computation complexity.

Proof of Theorem 2

Proof. We continue at Equation (13). Since $\mathbb{E}_{\mathbf{x} \sim \mathbb{X}}$ is the expectation with respect to the input space, we move the expectation inside the summation of RHS of Equation (13).

$$\mathbb{E}_{\mathbf{y} \sim \mathbb{Y}}\{\|\widetilde{\mathbf{y}} - \mathbf{y}\|_2^2\} = \sum_{i=1}^m \sum_{j=1}^m \mathbb{E}_{\mathbf{x} \sim \mathbb{X}}\{x_i x_j\} \mathbf{p}_i \mathbf{p}_j^T \quad (25)$$

Under Assumption 1, $\mathbb{E}_{\mathbf{x} \sim \mathbb{X}}\{x_i x_j\} = 0$ for $i \neq j$, the RHS of Equation (25) simplifies to:

$$\mathbb{E}_{\mathbf{y} \sim \mathbb{Y}}\{\|\widetilde{\mathbf{y}} - \mathbf{y}\|_2^2\} = \sum_{i=1}^m \mathbb{E}_{\mathbf{x} \sim \mathbb{X}}\{x_i^2\} \mathbf{p}_i \mathbf{p}_i^T \quad (26)$$

We can define diagonal matrix $\mathbf{S} = \text{diag}(\sqrt{\mathbb{E}_{\mathbf{x} \sim \mathbb{X}}\{x_1^2\}}, \sqrt{\mathbb{E}_{\mathbf{x} \sim \mathbb{X}}\{x_2^2\}}, \dots, \sqrt{\mathbb{E}_{\mathbf{x} \sim \mathbb{X}}\{x_m^2\}})$ and rewrite the RHS of Equation (26) as:

$$\mathbb{E}_{\mathbf{y} \sim \mathbb{Y}}\{\|\widetilde{\mathbf{y}} - \mathbf{y}\|_2^2\} = \text{Tr}(\mathbf{S} \mathbf{P} \mathbf{P}^T \mathbf{S}^T) = \|\mathbf{S} \mathbf{P}\|_F^2 \quad (27)$$

where $\text{Tr}(\cdot)$ denotes the trace of a matrix.

Therefore, the objective of Problem 2 (Equation (8)) is equivalent to:

$$\begin{aligned} \arg \min_{\mathbf{C}_k} \mathbb{E}_{\mathbf{y} \sim \mathbb{Y}}\{\|\widetilde{\mathbf{y}} - \mathbf{y}\|_2^2\} &= \arg \min_{\mathbf{C}_k} \|\mathbf{S} \mathbf{P}\|_F^2 \\ &= \arg \min_{\mathbf{C}_k} \|\mathbf{S}(\widetilde{\mathbf{W}} + \mathbf{C}_k - \mathbf{W})\|_F^2 \end{aligned} \quad (28)$$

TABLE V: Learning rates of RoBERTa-base experiments on GLUE.

Rank	W-bits	Method	Learning rates
-	16	Full FT	7e-5, 5e-5, 2e-5
8	16	LoRA	1e-4, 2e-4, 3e-4
8	4.25	QLoRA/LoftQ/QERA-approx	1e-4, 2e-4, 3e-4
8	3.25	QLoRA/LoftQ/QERA-approx	1e-4, 2e-4, 3e-4
64	2.50	QLoRA/LoftQ/QERA-exact	2e-5, 3e-5, 4e-5, 5e-5, 6e-5, 9e-5, 1e-4

If we assign $\mathbf{Q} = \mathbf{S}(\mathbf{W} - \widetilde{\mathbf{W}})$ and $\mathbf{Q}_k = \mathbf{S}\mathbf{C}_k$, the objective becomes:

$$\arg \min_{\mathbf{Q}} \|\mathbf{Q}_k - \mathbf{Q}\|_F^2 \quad (29)$$

Note that the invertible matrix \mathbf{S} in \mathbf{Q}_k does not change the rank of the matrix \mathbf{C}_k . According to the Eckart-Young-Mirsky theorem, the optimal rank k approximation to \mathbf{Q} is the truncated SVD of \mathbf{Q} :

$$\mathbf{Q}_k = \mathbf{U}_{:,k} \mathbf{\Sigma}_{:,k} \mathbf{V}_{:,k}^T \quad (30)$$

where $\mathbf{U}\mathbf{\Sigma}\mathbf{V}^T = \text{SVD}(\mathbf{Q}) = \text{SVD}(\mathbf{S}(\mathbf{W} - \widetilde{\mathbf{W}}))$.

Finally, we get the optimal solution to the low-rank term \mathbf{C}_k :

$$\mathbf{C}_k = \mathbf{S}^{-1} \mathbf{Q}_k = \mathbf{S}^{-1} \mathbf{U}_{:,k} \mathbf{\Sigma}_{:,k} \mathbf{V}_{:,k}^T \quad (31)$$

□

C. Detailed Experiment Setup

We mainly use PyTorch, Transformers, PEFT, and Accelerate to implement QERA. We use SciPy’s implementation of blocked Schur algorithm [36] to calculate the matrix square root, which runs on CPUs. The evaluation is performed with lm-evaluation-harness, Evaluate, and AlpacaEval 2.0 [35].

1) *QPEFT Hyperparameters*: We perform fine-tuning experiments on four NVIDIA A100 80GB GPUs with AMD EPYC 64-Core Processor with 1024GB RAM. The total fine-tuning time is around 2100 GPU hours.

a) *RoBERTa-base on GLUE*: We sweep learning rates for each baseline/method, and collect the best accuracy. The reported accuracy is the average value across random seeds 42, 1, and 2. The total batch size is 64 for all GLUE experiments and we train the models for 5 epochs. For 4-bit experiments, we use 4-bit floating point from the QLoRA implementation in PEFT. For 3-bit experiments, we use emulated MXINT [37] with block size = 32 and for 2-bit experiments we use MXINT with block size = 16. Table V lists the learning rates for each experiment.

b) *LLaMA-2-7B/-3.1-8B on SlimPajama and GSM8K*: We adopt the learning rates in (author?) [38]. The reported perplexity/accuracy is the average value across random seeds 42, 1, and 2. For SlimPajama, we fine-tune the model on a subset for 1000 steps with rank = 8, total batch size = 64, sequence length = 1024, learning rate = 3e-5. For GSM8K, we fine-tune the model for 10 epochs with rank = 64, total batch size = 128, sequence length = 384, and learning rate = 3e-5.

2) *PTQ Hyperparameters*: We perform PTQ experiments on eight NVIDIA A6000 48GB GPUs with AMD EPYC 256-Core Processor with 1024GB RAM. The total quantization and evaluation time is around 4500 GPU hours. We report 0-shot accuracy or normalized accuracy (if available) for all tasks except WikiText2, in which we report word perplexity. The sequence length for reporting word perplexity is the model’s context length by default, except for Phi-3.5 and LLaMA-3.1. For these two models, we set the sequence length = 2048. We use the HuggingFace Transformers’s implementation of HQQ, and reimplement ZeroQuant-V2 and LQER as baselines. We use MXINT with block size = 32 as the quantization format for all quantization methods except HQQ, which uses its built-in INT format with group size = 64. Thus, both formats have an average W-bits of 4.25. We evaluate quantized Vicuna-v1.5-7B, which is an instruction-tuned LLaMA-2-7B, with AlpacaEval 2.0. and use GPT4-Turbo as the evaluator. The reported win rate is the length-controlled win rate, which is a debiased version of the win rate that controls for the length of the generated outputs.

D. Decreasing Weight Error \neq Decreasing Output Error for LoftQ

We provide the weight approximation error, $\|\mathbf{W} - \widetilde{\mathbf{W}} - \mathbf{C}_k\|_F$, in Figure 6, of all linear layers in RoBERTa-base by sweeping the number of iterations. We observe that the weight approximation error monotonically decreases with the number of iterations, but as shown in Figure 1, the model output error may increase. This observation indicates that the commonly used objective of minimizing the weight approximation error and the corresponding algorithm are not ideal for the quantization error reconstruction problem.

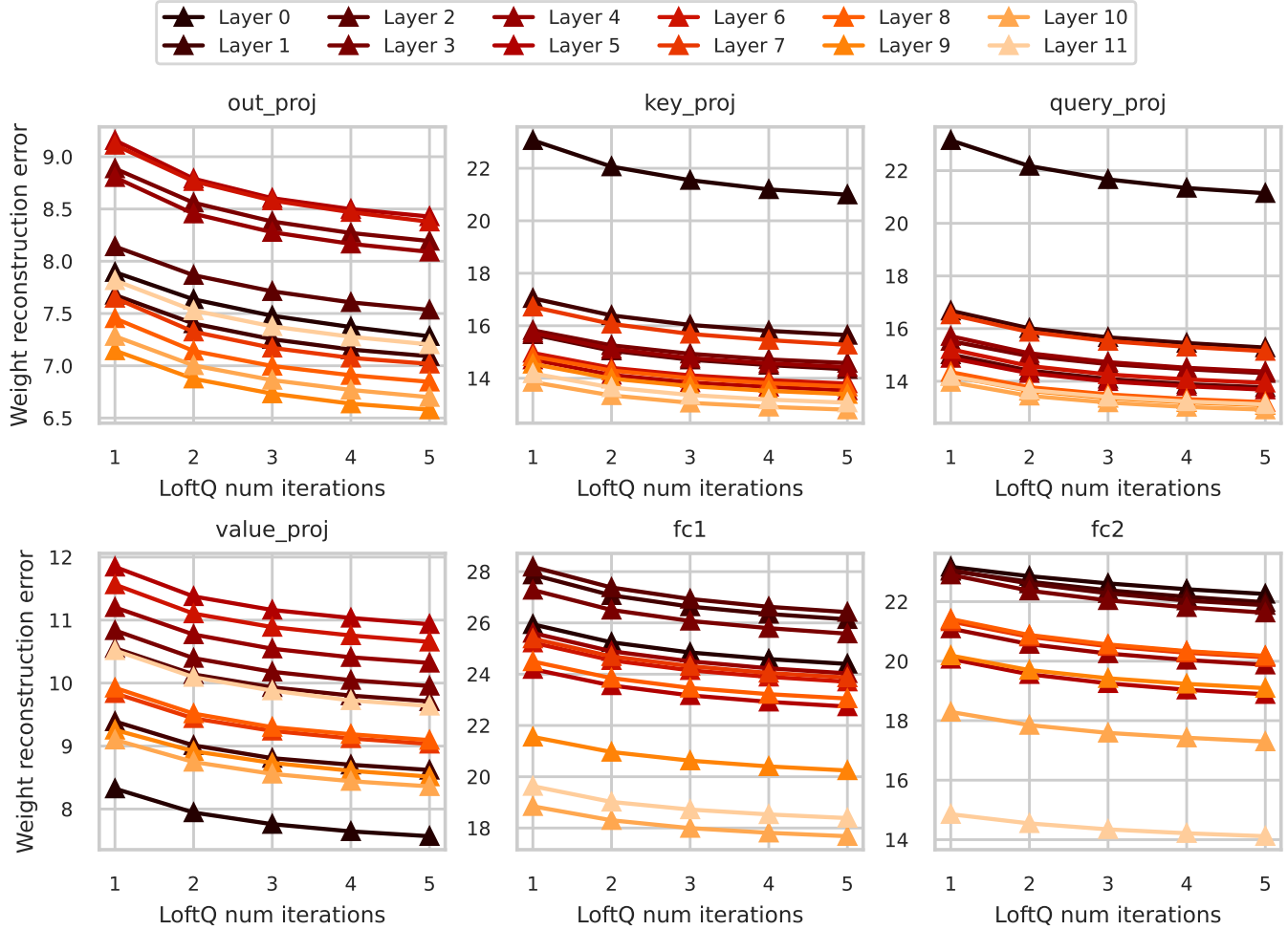


Fig. 6: Weight approximation error of 3-bit rank-16 LoftQ with different numbers of iterations on RoBERTa-base. We observe that the weight reconstruction error of all the layers decreases as the number of iterations increases, but as shown in Figure 1b, the model output error ($k=16$) increases from the 4-th to 5-th iteration.

E. Test of Assumption 1

We provide more plots of normalized \mathbb{R}_{XX} magnitude, $\frac{\text{abs}(\mathbb{R}_{XX})}{\|\mathbb{R}_{XX}\|_F}$, in Figures 7 to 10, where dark pixels are elements close to zeros. There are strongly correlated embedding channels in some k_{proj} and o_{proj} layers. The assumption fits better in MLP layers (gate_proj, up_proj, and down_proj).

F. Choice of Calibration Set

We compare the QERA-adapted models calibrated on the pretraining dataset and the downstream dataset. Specifically, we fine-tune two QERA-adapted 2-bit RoBERTa-base models. One is calibrated on its pretraining dataset, WikiText2, and the other on SST2. Figure 11 shows the loss curves of the two models across three learning rates. None loss curves of the models calibrated on SST2 decreases, but the ones calibrated on WikiText2 successfully decrease and converge. We hypothesize that this is due to the massive padding tokens in preprocessed SST2 considering that the raw sample lengths change fiercely. However, WikiText2 samples were preprocessed in the masked language modeling style, which means that only a few special tokens are added to the grouped texts.

G. Scalability and Numerical Stability of QERA

One may notice the diminishing model performance improvement of QERA-exact over QERA-approx as the model size increases. The main reason is that larger LLMs are more resistant to quantization [39]. Another reason can be the error ratio of the matrix square root calculation of the autocorrelation matrix increases with model hidden size (Figure 12a).

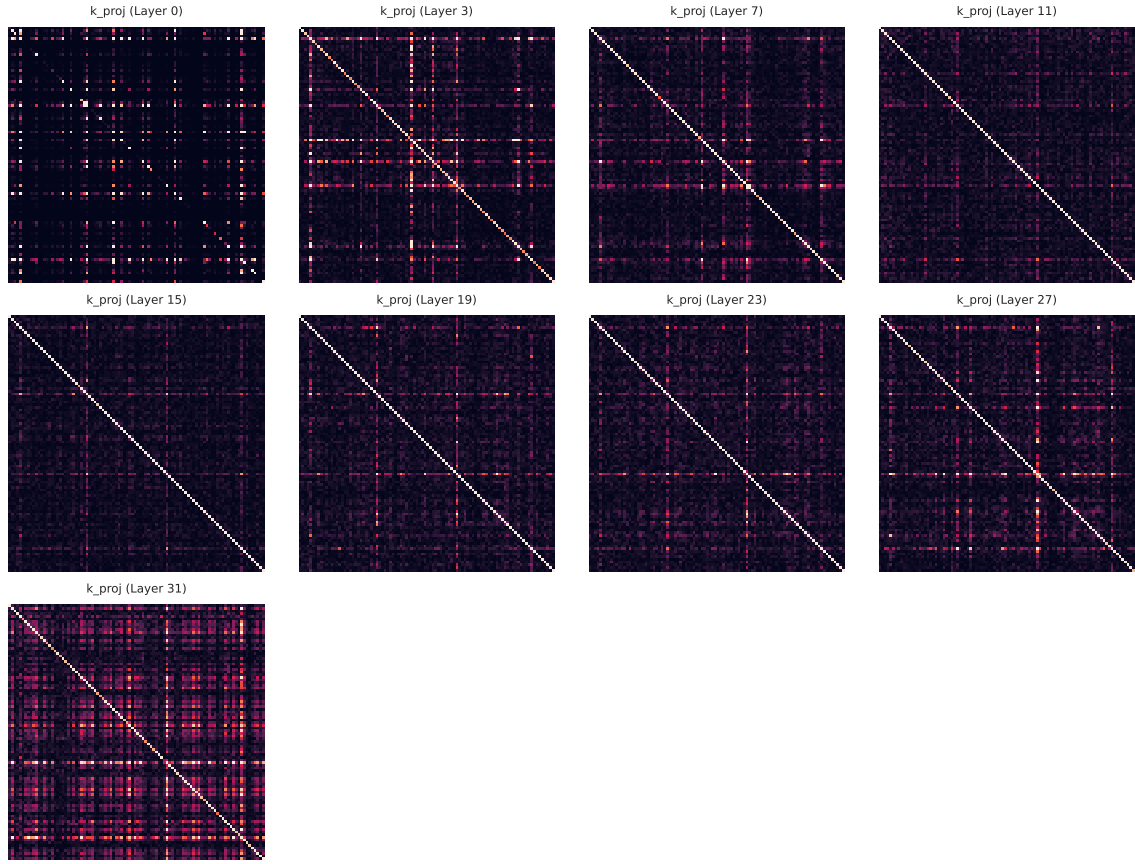


Fig. 7: Normalized $\text{abs}(\mathbb{R}_{\text{XX}})$ of inputs of k_proj layers in LLaMA-3-8B. Note that the q_proj and v_proj share the same inputs. Layers are sampled and only the first 96 dimensions are plotted for clarity.

We find that the data type used in the calibration is important for the numeric stability of QERA-exact due to the calculation of the matrix square root and SVD. To improve the stability of the calculation in QERA-exact, a good practice we find is to perform the outer product of \mathbb{R}_{XX} in FP32, accumulated outer product in FP64, and calculate the matrix square root in FP64 using the blocked Schur algorithm [36]. Figure 12b illustrates the quantization time of QERA-approx and QERA-exact on the platform described in Appendix C where the linear layers are quantized sequentially. QERA-exact is slow due to the calculation of matrix square roots on CPUs. GPU-accelerated matrix square root will be the key optimization to reduce the quantization time. Note that in QERA, the quantization of individual layers is independent, allowing more parallelization and acceleration of the quantization process.

H. Choices of LoRA Ranks and Models

a) *Rank = 8 for GLUE experiments*: We notice LoftQ paper uses a large rank of 16 and 32 for fine-tuning on GLUE, which is larger than the commonly-used rank value of LoRA (4 or 8 in LoRA paper [12]). If we consider LoRA as the upper limit of QLoRA-like QPEFT methods (including LoftQ and QERA), to effectively compare these QPEFT methods, one easy way is to set the rank as the minimum value required by LoRA and check which QPEFT method achieves an accuracy closest to LoRA. This is why we choose rank = 8 for GLUE experiments (For 2-bit GLUE experiments we use a large rank 64 since the quantization is very aggressive). If we use rank = 32, LoRA and all the QPEFT methods may be over-parameterized and it will be hard to make a fair comparison in terms of fine-tuned accuracy.

b) *RoBERTa vs. DeBERTa*: When investigating the related work, we find that both RoBERTa and DeBERTaV3 [40] are used in QPEFT experiments [3, 1, 38, 3, 41]. The reason why we chose RoBERTa is that the RoBERTa checkpoint on HuggingFace² is complete and compatible with both HuggingFace’s official examples of sequence classification³ and masked language modeling⁴. Specifically, the RoBERTa checkpoint contains both the base model and the masked language modeling

²RoBERTa-base checkpoint: link

³HuggingFace example of sequence classification: link

⁴HuggingFace example of masked language modeling: link

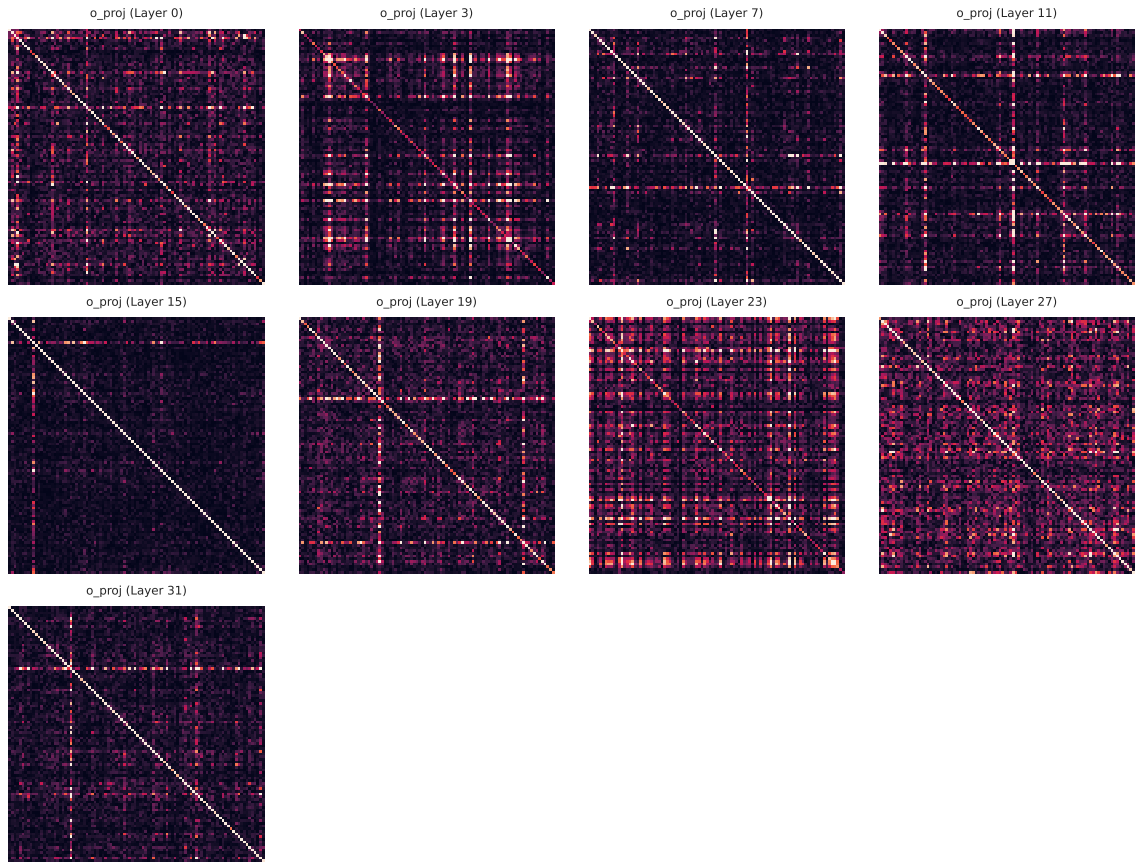


Fig. 8: Normalized $\text{abs}(\mathbb{R}_{\text{XX}})$ of inputs of o_proj layers in LLaMA-3-8B. Layers are sampled and only the first 96 dimensions are plotted for clarity.

head but the DeBERTaV3’s checkpoint⁵ only contains the base model. As we know, the base model is enough for fine-tuning on downstream tasks. However, to calibrate on the pretraining dataset, we need the language modeling head to verify if our implementation of data preprocessing and calibration matches how the model was originally pretrained. Note that the quality of the statistic values in QERA like \mathbb{R}_{XX} depends on the quality of the calibration set. Thus, without the language modeling head in the checkpoint, we cannot perform the QERA’s calibration for DeBERTaV3 properly, ensure the correctness of statistics in QERA, and explore the effect of the choice of calibration sets.

I. Detailed PTQ Results

Here we offer the detailed evaluation results for each downstream task in Tables VI to XII.

TABLE VI: Post-training quantization evaluation of TinyLlama-1.1B.

rank	Method	w-bits	ARC (challenge)	BoolQ	CommonSenseQA	BBH	MMLU	WikiText2	Winogrande
			Acc_norm	Acc	Acc	Acc_norm	Acc	Word ppl	Acc
32	BF16	4.25	32.51	55.93	20.07	29.68	25.35	13.98	59.59
	HQQ		32.00	58.13	20.15	29.70	25.75	15.02	59.35
	w -only		28.67	58.23	19.49	28.99	23.81	19.40	52.01
	ZeroQuant-V2		29.69	57.86	19.41	29.53	24.85	18.03	52.57
	LQER		32.00	52.42	18.59	29.60	25.31	16.23	59.75
	QERA-approx		31.83	52.08	17.20	29.51	25.22	15.66	58.72
	QERA-exact		32.00	51.31	19.33	29.42	25.19	16.16	59.67

⁵DeBERTaV3’s checkpoint: [link](#)

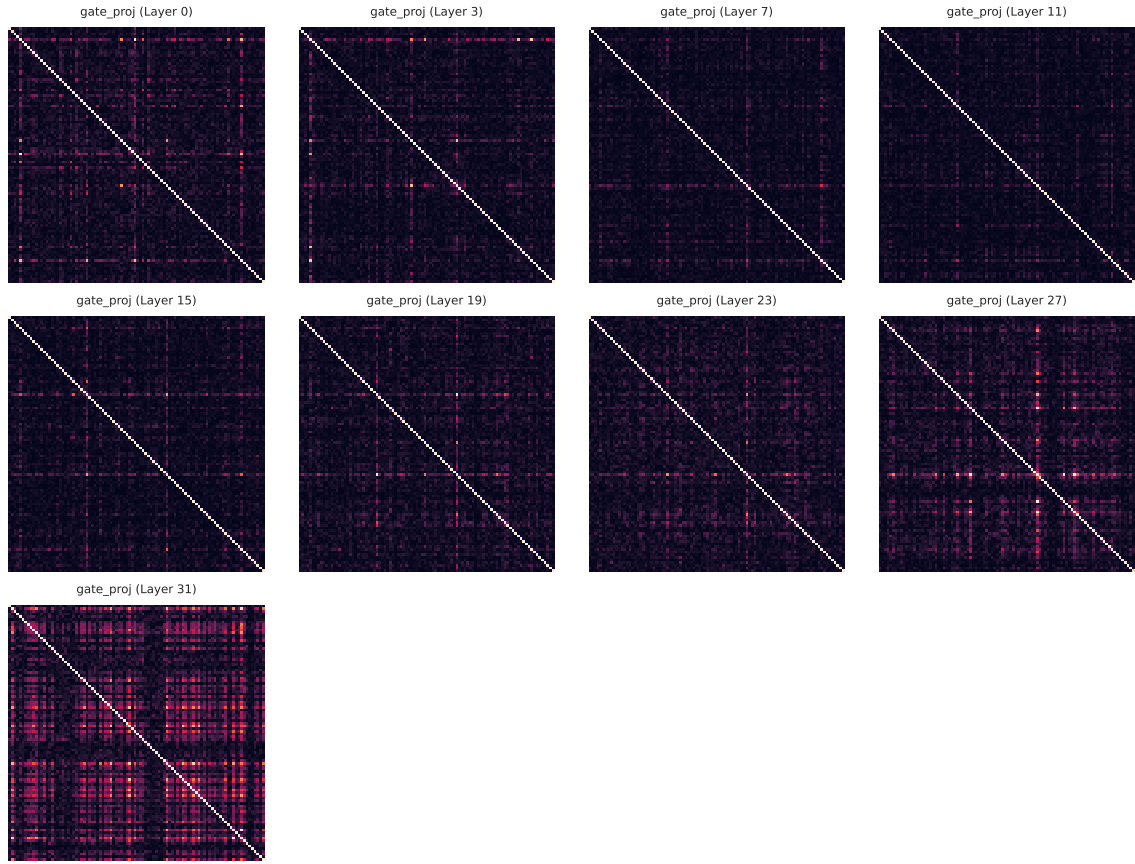


Fig. 9: Normalized $\text{abs}(\mathbb{R}_{\text{XX}})$ of inputs of `gate_proj` layers in LLaMA-3-8B. Note that the `up_proj` shares the same inputs. Layers are sampled and only the first 96 dimensions are plotted for clarity.

TABLE VII: Post-training quantization evaluation of Gemma-2-2B.

rank	Method	W-bits	ARC (challenge)	BoolQ	CommonSenseQA	BBH	MMLU	WikiText2	Winogrande
			Acc_norm	Acc	Acc	Acc_norm	Acc	Word ppl	Acc
32	BF16	4.25	49.91	72.60	50.29	32.67	49.44	13.08	68.82
	HQQ		48.81	71.77	48.40	32.32	46.52	14.29	67.40
	w-only		44.62	69.91	34.07	31.96	42.90	16.23	66.54
	ZeroQuant-V2		44.45	69.94	34.07	31.50	43.27	15.71	66.22
	LQER		46.08	68.84	37.59	32.60	45.78	14.55	67.72
	QERA-approx		45.31	68.99	36.20	32.04	45.80	14.60	67.40
	QERA-exact		46.84	72.32	42.75	33.36	47.29	14.12	67.80

TABLE VIII: Post-training quantization evaluation of Phi3-3.5-mini.

rank	Method	W-bits	ARC (challenge)	BoolQ	CommonSenseQA	BBH	MMLU	WikiText2	Winogrande
			Acc_norm	Acc	Acc	Acc_norm	Acc	Word ppl	Acc
32	BF16	4.25	59.39	84.65	71.91	48.19	64.58	11.50	72.77
	HQQ		57.00	74.34	60.20	38.22	56.00	14.63	69.61
	w-only		59.73	82.72	68.22	44.45	61.54	14.16	70.48
	ZeroQuant-V2		59.64	82.94	68.06	44.58	62.00	14.09	69.77
	LQER		59.39	84.01	70.76	45.67	62.21	12.88	70.74
	QERA-approx		59.45	84.82	70.84	45.67	62.26	12.81	70.17
	QERA-exact		58.70	83.73	69.45	45.37	62.01	13.00	71.19

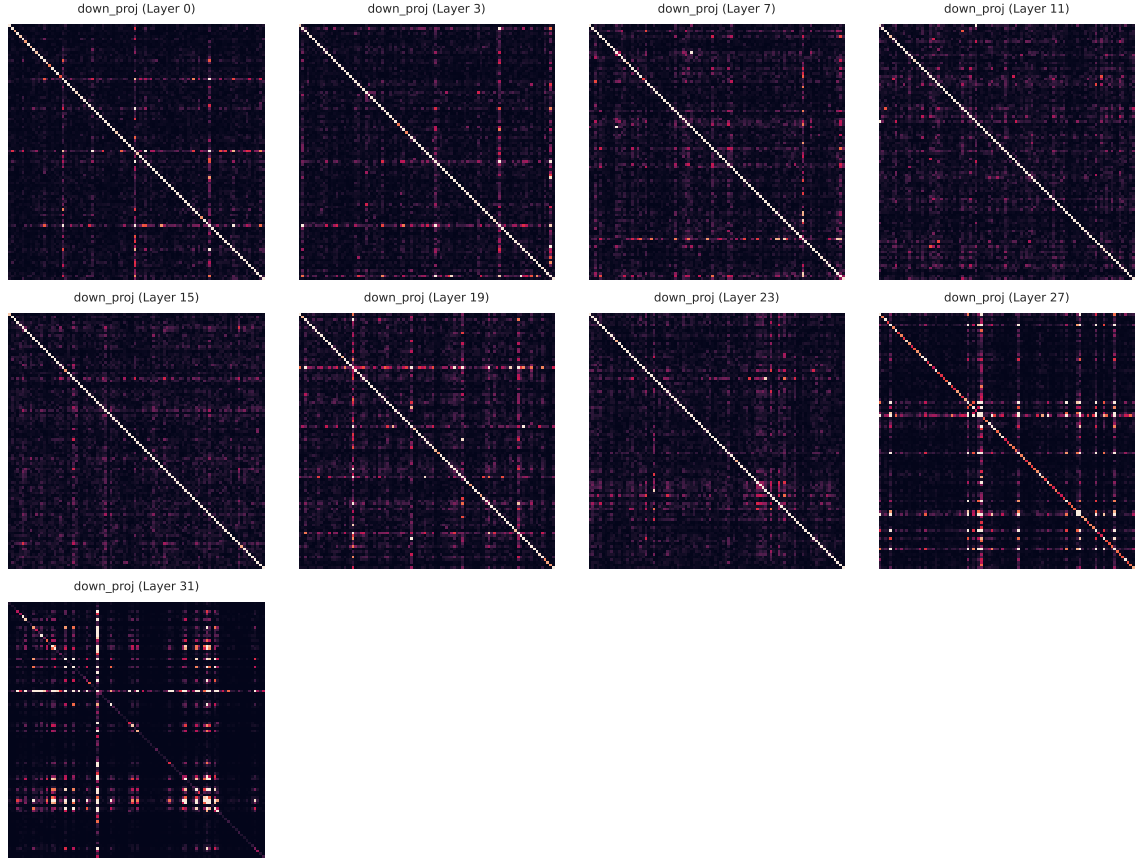


Fig. 10: Normalized $\text{abs}(\mathbb{R}_{\mathbf{X}\mathbf{X}})$ of inputs of `down_proj` layers in LLaMA-3-8B. Layers are sampled and only the first 96 dimensions are plotted for clarity.

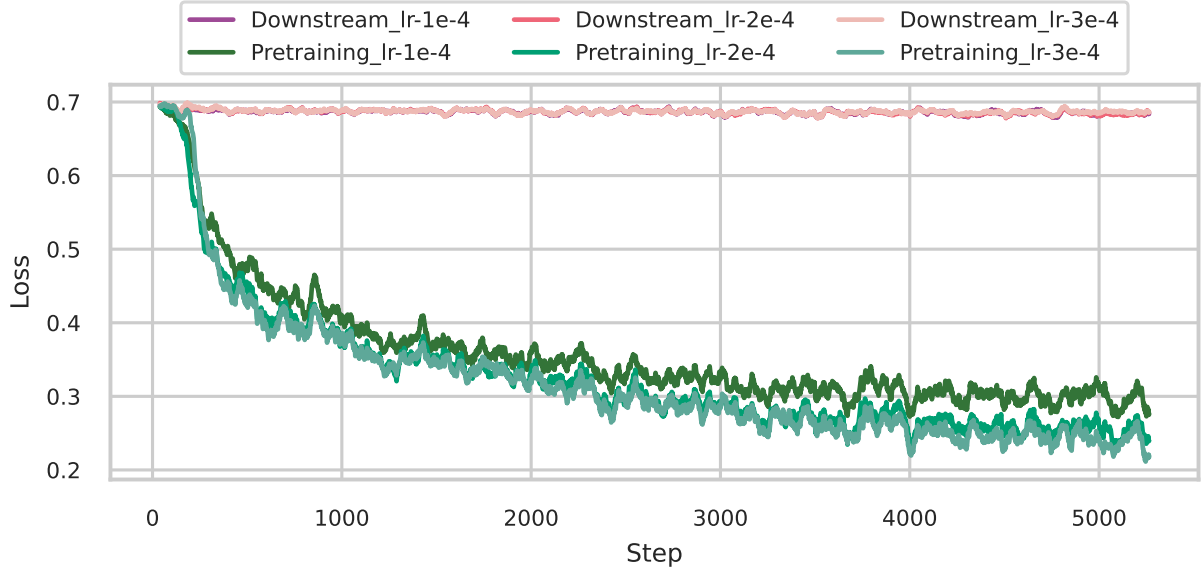
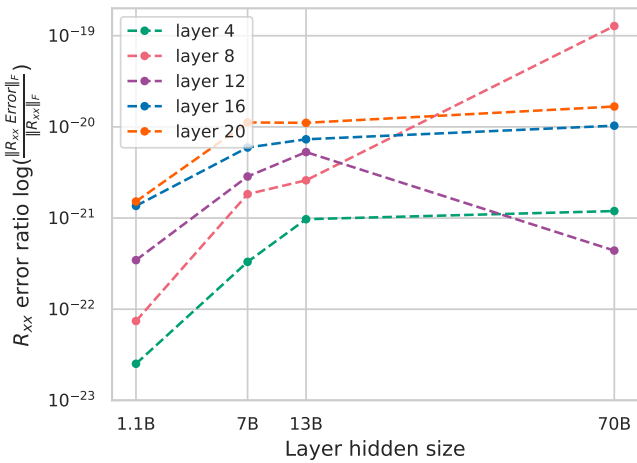
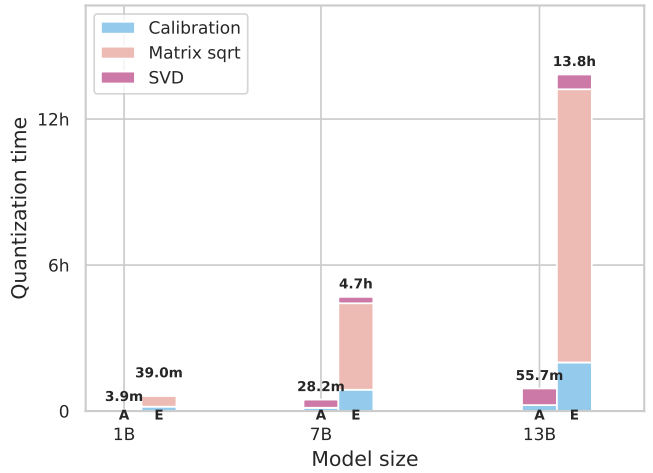


Fig. 11: The fine-tuning loss curves of QERA-adapted 2-bit RoBERTa-base on SST2. The loss fails to decrease if the calibration is performed on the downstream task SST2 due to the massive padding tokens in preprocessed SST2 samples. In pretraining dataset, there are only a few special tokens like padding tokens and mask tokens.



(a) Estimated error ratio of the square root of \mathbb{R}_{xx}



(b) QERA quantization time

Fig. 12: Scalability of QERA. (a) plots the estimated error ratio of the matrix square root calculation of \mathbb{R}_{xx} of some layers where the error increases as the model goes larger. (b) compares the quantization time of QERA-approx and QERA-exact if all layers are quantized sequentially. The matrix square root is time-consuming since it is executed on CPUs. One key optimization for accelerating the quantization process of QERA-exact will be the GPU-accelerated matrix square root.

TABLE IX: Post-training quantization evaluation of LLaMA-2-7B.

rank	Method	W-bits	ARC (challenge)	BoolQ	CommonSenseQA	BBH	MMLU	WikiText2	Winogrande
			Acc_norm	Acc	Acc	Acc_norm	Acc	Word ppl	Acc
32	BF16	4.25	46.25	77.83	33.09	30.74	40.64	8.71	69.14
	HQQ		44.03	75.87	29.40	30.50	40.14	9.59	69.61
	w-only		45.22	75.87	25.47	30.71	40.03	9.45	68.43
	ZeroQuant-V2		45.82	75.90	24.82	29.99	39.84	9.42	68.19
	LQER		44.28	76.15	29.81	30.72	40.66	9.22	69.22
	QERA-approx		44.28	75.96	30.96	30.72	40.59	9.17	68.59
	QERA-exact		44.80	76.39	31.61	30.57	40.86	9.12	69.22

TABLE X: Post-training quantization evaluation of LLaMA-2-13B.

rank	Method	W-bits	ARC (challenge)	BoolQ	CommonSenseQA	BBH	MMLU	WikiText2	Winogrande
			Acc_norm	Acc	Acc	Acc_norm	Acc	Word ppl	Acc
32	BF16	4.25	49.49	80.58	47.34	32.65	52.18	7.68	72.22
	HQQ		49.06	78.69	45.05	32.41	50.85	8.27	71.11
	w-only		50.43	80.58	44.06	33.45	50.21	8.06	71.98
	ZeroQuant-V2		50.00	81.04	44.47	33.50	50.31	8.07	71.59
	LQER		51.02	81.25	44.47	32.41	51.24	7.96	71.98
	QERA-approx		51.11	80.83	44.06	32.48	51.07	7.95	71.67
	QERA-exact		50.77	81.10	44.55	32.91	51.23	7.93	71.98

TABLE XI: Post-training quantization evaluation of LLaMA-3.1-8B.

rank	Method	W-bits	ARC (challenge)	BoolQ	CommonSenseQA	BBH	MMLU	WikiText2	Winogrande
			Acc_norm	Acc	Acc	Acc_norm	Acc	Word ppl	Acc
32	BF16	4.25	53.50	82.05	71.42	39.07	63.27	7.55	73.95
	HQQ		52.73	81.19	69.86	35.60	62.14	8.72	74.03
	w-only		50.68	81.31	67.24	37.34	59.03	8.78	73.56
	ZeroQuant-V2		51.11	81.25	66.99	38.43	58.94	8.83	73.48
	LQER		50.34	80.98	67.49	38.05	60.23	8.45	73.40
	QERA-approx		50.77	81.04	66.75	37.94	60.09	8.45	73.48
	QERA-exact		51.28	80.18	68.83	37.48	60.60	8.33	73.95

TABLE XII: Post-training quantization evaluation of LLaMA-3.1-70B.

rank	Method	W-bits	ARC (challenge)	BoolQ	CommonSenseQA	BBH	MMLU	WikiText2	Winogrande
			Acc_norm	Acc	Acc	Acc_norm	Acc	Word ppl	Acc
32	BF16	4.25	65.10	85.38	78.46	48.53	75.28	3.06	79.56
	HQQ		63.99	85.02	77.48	48.19	75.20	3.97	77.98
	w-only		60.58	83.82	73.63	41.28	73.06	4.55	78.37
	ZeroQuant-V2		59.90	83.61	73.55	42.75	73.15	4.48	77.74
	LQER		62.97	83.88	76.25	48.67	74.26	4.10	79.64
	QERA-approx		62.12	83.79	76.74	48.53	73.98	4.10	79.64